

AD-A045 112

HARVARD UNIV CAMBRIDGE MASS DIV OF ENGINEERING AND --ETC F/G 20/12
A STRUCTURAL MODEL FOR THE INTERFACE BETWEEN AMORPHOUS AND CRYST--ETC(U)
JUL 77 F SPAEPEN

N00014-77-C-0002

NL

UNCLASSIFIED

TR-2

1 of 1
ADA045112



END
DATE
FILMED
11-77
DDC

ADA 045 112

Handwritten marks: a circled '15', a circled '11', and a large stylized '11' in a circle.

15 Office of Naval Research

Contract N00014-77-C-0002, MR-039-136

National Science Foundation Grant NSF-DMR76-0111

6 A STRUCTURAL MODEL FOR THE INTERFACE BETWEEN AMORPHOUS AND CRYSTALLINE Si OR Ge



DDC PREPARED OCT 5 1977

By

10 Frans Spaepen

11 Jul 1977

12 367.

9 Technical Report No. 2

14 TR-2

This document has been approved for public release and sale; its distribution is unlimited. Reproduction in whole or in part is permitted by the U. S. Government.

AD No. DDC FILE COPY

Division of Applied Sciences Harvard University Cambridge, Massachusetts

163 750

mt

Unclassified

SECURITY CLASSIFICATION OF THIS PAGE (When Data Entered)

REPORT DOCUMENTATION PAGE		READ INSTRUCTIONS BEFORE COMPLETING FORM
1. REPORT NUMBER Technical Report No. 2	2. GOVT ACCESSION NO.	3. RECIPIENT'S CATALOG NUMBER
4. TITLE (and Subtitle) A STRUCTURAL MODEL FOR THE INTER- FACE BETWEEN AMORPHOUS AND CRYSTALLINE Si OR Ge	5. TYPE OF REPORT & PERIOD COVERED Interim Report	
	6. PERFORMING ORG. REPORT NUMBER	
7. AUTHOR(s) Frans Spaepen	8. CONTRACT OR GRANT NUMBER(s) N00014-77-C-0002 NSF DMR76-0111	
9. PERFORMING ORGANIZATION NAME AND ADDRESS Division of Applied Science Harvard University Cambridge, MA 02138	10. PROGRAM ELEMENT, PROJECT, TASK AREA & WORK UNIT NUMBERS	
11. CONTROLLING OFFICE NAME AND ADDRESS	12. REPORT DATE July 1977	13. NUMBER OF PAGES 35
	14. MONITORING AGENCY NAME & ADDRESS (if different from Controlling Office)	
15. SECURITY CLASS. (of this report) Unclassified		15a. DECLASSIFICATION/DOWNGRADING SCHEDULE
16. DISTRIBUTION STATEMENT (of this Report) This document has been approved for public release and sale; its distribution is unlimited. Reproduction in whole or in part is permitted by the U.S. Government.		
17. DISTRIBUTION STATEMENT (of the abstract entered in Block 20, if different from Report)		
18. SUPPLEMENTARY NOTES		
19. KEY WORDS (Continue on reverse side if necessary and identify by block number) Amorphous Ge and Si Phase boundary Static structural model Crystallization Surface tension		
20. ABSTRACT (Continue on reverse side if necessary and identify by block number) A general procedure for building static models of interfaces, which involves a change in phase-specific construction rules at the boundary plane, is outlined. Its application to tetrahedrally coordinated materials shows that an amorphous-crystalline interface model can be created by replacing the 'chair'-type sixfold rings (typical of the crystal) by a mixture of different ones (typical of the amorphous phase). The interface consists of two crystalline and two amorphous layers. The detailed topologies, bond angle distortions, and		

DDC
APPROVED
OCT 5 1977
RECEIVED
C

DD FORM 1473 1 JAN 73

EDITION OF 1 NOV 65 IS OBSOLETE
S/N 0102-014-6601

Unclassified

SECURITY CLASSIFICATION OF THIS PAGE (When Data Entered)

20. Abstract continued

radial distribution functions for each of the four layers are reported. The surface tension has a large energetic component due to the excess strain energy in both the amorphous and crystalline interface layers. For Ge the estimated surface tension is 0.235 J m^{-2} . This is used to show that the model, which contains no dangling bonds, represents a state of minimum energy. Application to the problem of creating a model for amorphous Ge by connecting randomly oriented crystallites with a random network matrix shows that such a model consists of more than 80% random network. Finally it is pointed out that the interface model is a starting point for a detailed description of the crystallization process.



* 0.235 J / sq M

ACCESSION for	on <input checked="" type="checkbox"/>
NTIS	on <input type="checkbox"/>
DDC	on <input type="checkbox"/>
UNANNOUNCED	
JUL 1 1971	
BY	
DISTRIBUTION/AVAILABILITY CODES	
DI	SPECIAL
A	

Office of Naval Research
Contract N00014-77-C-0002 NR-039-136
National Science Foundation Grant DMR76-0111

A STRUCTURAL MODEL FOR THE INTERFACE
BETWEEN AMORPHOUS AND CRYSTALLINE Si OR Ge

By
Frans Spaepen

Technical Report No. 2

This document has been approved for public release
and sale; its distribution is unlimited. Reproduction in
whole or in part is permitted by the U. S. Government.

July 1977

The research reported in this document was made possible through
support extended the Division of Applied Science, Harvard University,
by the Office of Naval Research, under Contract N00014-77-C-0002.

Division of Applied Science
Harvard University . Cambridge, Massachusetts

ABSTRACT

A general procedure for building static models of interfaces, which involves a change in phase-specific construction rules at the boundary plane, is outlined. Its application to tetrahedrally coordinated materials shows that an amorphous-crystalline interface model can be created by replacing the 'chair'-type sixfold rings (typical of the crystal) by a mixture of different ones (typical of the amorphous phase). The interface consists of two crystalline and two amorphous layers. The detailed topologies, bond angle distortions and radial distribution functions for each of the four layers are reported. The surface tension has a large energetic component due to the excess strain energy in both the amorphous and crystalline interface layers. For Ge the estimated surface tension is 0.235 J m^{-2} . This is used to show that the model, which contains no dangling bonds, represents a state of minimum energy. Application to the problem of creating a model for amorphous Ge by connecting randomly oriented crystallites with a random network matrix shows that such a model consists of more than 80% random network. Finally it is pointed out that the interface model is a starting point for a detailed description of the crystallization process.

INTRODUCTION

The crystallization of amorphous Si and Ge is a phenomenon of considerable scientific and technological interest. Recent investigations have shown that amorphous Ge crystallizes in the range 300-400°C, and the reported activation energies range from 1.4 eV - 3.5 eV (Barna, Barna and Pocza, 1972; Germain, Squelard, Bourgoïn and Gheorghiu, 1975; Chik and Lim, 1975). Since specimen contamination in evaporated samples has a strong effect on the crystallization temperature and kinetics, special attention should be paid to results obtained from re-growth in amorphous Ge and Si layers produced by ion implantation of single crystals, since this technique produces very clean samples. The activation energy for crystallization in such samples is 2.0 eV for Ge (Csepregi, Kullen, Mayer and Sigmon, 1977) and 2.3 eV for Si, which crystallizes in the range 500-600°C (Csepregi, Mayer and Sigmon, 1975). All investigators agree that the magnitude of the activation energy must be explained by the formation of some intermediary defect in the amorphous-crystalline boundary during crystallization. The proposals on the nature of this defect vary from monovacancies (Csepregi, Kullen, Mayer and Sigmon, 1977), divacancies (Bourgoïn and Germain, 1975), to extended divacancies (Chik and Lim, 1975). The major problem in sorting out the exact nature of this defect is the lack of knowledge about the topology of the interface structure. Therefore, in this paper a model for the amorphous-crystalline boundary in these materials will be proposed which allows detailed insight into the interface topology. As yet, no attempt will be made to describe the crystallization process

using this model, but it will provide a useful starting point to explain not only the observed activation energy but also the prefactor of the process.

GENERAL REMARKS ON THE CONSTRUCTION OF STATIC MODELS FOR INTERFACES

The interface between two phases of a one-component system is, at any given temperature and pressure, inherently unstable: the system can always lower its free energy by removing the interface and by converting to the more stable or, at equilibrium, either one of the two phases. This is obviously a problem when one wants to construct a structural model of the interface. The only completely rigorous, but cumbersome and expensive, approach to the problem is a molecular dynamics calculation on a steady state system in a small temperature or pressure gradient which stabilizes a different phase on the opposite sides of the system. (The steady state requires that a continuous flow of heat or matter is maintained.) Such a calculation would provide a complete model of planar interface in dynamic equilibrium.

An alternative approach is that of building static models by hand or with the aid of the computer. This method does not produce an equilibrium system (a static model can be considered to be at 0°K), and hence lacks the rigor of molecular dynamics. Its advantages, however, are inexpensiveness, ease of construction, and the simple physical insight it provides into the topological problem of connecting the two phases.

One way to obtain a static model of a planar interface is by first building one of the bulk phases to one side of a geometrical plane (or in other words: imagine a planar cut through the homogeneous bulk

phase, and removal of the material on one side). The construction is then continued on the other side of the plane, but a new set of construction rules, related to the structure of the bulk second phase rather than the first one, is used. If the construction rules from the second phase can be used with a plane boundary condition determined by the first phase, the structure of the subsequently added interfacial layers will gradually change, until finally the structure of the bulk second phase is reached. Such a match between the two structures should produce, if necessary after some additional local relaxation, an interface with a minimum excess energy.

It must be emphasized that this change of phase-specific construction rules at the boundary plane is an absolutely necessary feature in the construction of the static interface models. The use of more general construction principles, e. g. , energy based rules, such as density maximization or distortion minimization, just leads to a continuation of the first phase beyond the boundary plane, since such general principles are common to construction of both phases. The main problem, therefore, is the choice of the appropriate phase-specific construction rules.

The most straightforward case is that involving only crystalline phases, since they are characterized completely by their lattice translation vectors. For an interface between two identical crystals of different orientation, the phase-specific rule which changes across the boundary plane is simply the orientation of the lattice vectors. It can be seen that in this case the approach outlined above leads to the construction of the symmetrical coincidence grain boundary (Gleiter and Chalmers, 1972).

When one of the phases is amorphous, the choice of the phase-specific rules is less obvious, and is in fact only possible if detailed structural information about the amorphous phase is available. The dense random packing (DRP) of hard spheres, for example, is an amorphous system, the structure of which has been thoroughly investigated (Bernal, 1964; Finney, 1970). This structural information was the basis of a recently developed static model for the interface between a DRP and a close packed crystal of hard spheres (Spaepen, 1975; Spaepen and Meyer, 1976). The construction was started with the crystalline phase, since its structure is fully known and it can conveniently be terminated on a well-defined crystal plane, e. g. (111). It was then observed that the interstices in the crystal are tetrahedra and octahedra, periodically arranged according to a ratio 2/1; the DRP, on the other hand, contains mostly tetrahedral interstices and very few octahedral ones (ratio 15/1). The occurrence of octahedral interstices was therefore taken as a phase-specific rule for the crystal, and their disappearance, together with the preponderance of tetrahedra, as a phase-specific rule for the DRP. Further construction, following the earlier described procedure and using this change of rules, resulted in the disappearance of the crystal symmetry and a gradual decrease in the localization of the subsequently added interfacial layers, until finally the DRP structure was reached.

Since this approach to modeling the crystal-amorphous interface for a hard sphere system seemed to be successful, in the sense that it explained the available direct and indirect experimental observations, an attempt will be made here to use the same basic approach to model the crystal-amorphous interface for directionally bonded, tetrahedrally coordinated systems.

SELECTION OF THE PHASE-SPECIFIC CONSTRUCTION RULES

At ambient temperature and pressure, Si and Ge crystallize into the diamond cubic structure. It is convenient to describe this structure as a stacking of layers perpendicular to a $[111]$ direction, as shown in Fig. 2c. Each atom has 4 nearest neighbors (tetrahedrally arranged, i. e., the angle between adjoining nearest neighbor bonds is exactly $109^{\circ}28'$), 12 second-nearest neighbors at 1.63 times the nearest neighbor distance (N. N. D.), and 12 third-nearest neighbors at 1.92 N. N. D., as indicated on the radial distribution function of Fig. 1. Each atom has one nearest neighbor bond parallel to the particular $[111]$ direction chosen. The three other bonds form topologically two-dimensional networks, perpendicular to this direction. These layers are not quite planar, but puckered: atoms whose fourth bond connects to the layer above are located $1/3$ N. N. D. above those whose fourth bond connects to the layer below. It is easily seen on Fig. 2c that the layers are composed of puckered six-fold rings in these "chair" configurations. In fact, the crystal can be thought of as composed entirely of these chair-type rings, since it is also the only type that is formed between successive layers. The longest distance between atoms in one particular ring is the third-nearest neighbor distance (1.92 N. N. D.). The abundance of these chair-type rings, therefore, results in a strong peak at this distance in the radial distribution function (Fig. 1).

The structure of amorphous Si and Ge has been the object of thorough investigation for the first half of this decade. By now, it has become clear that the structure can be most satisfactorily described by

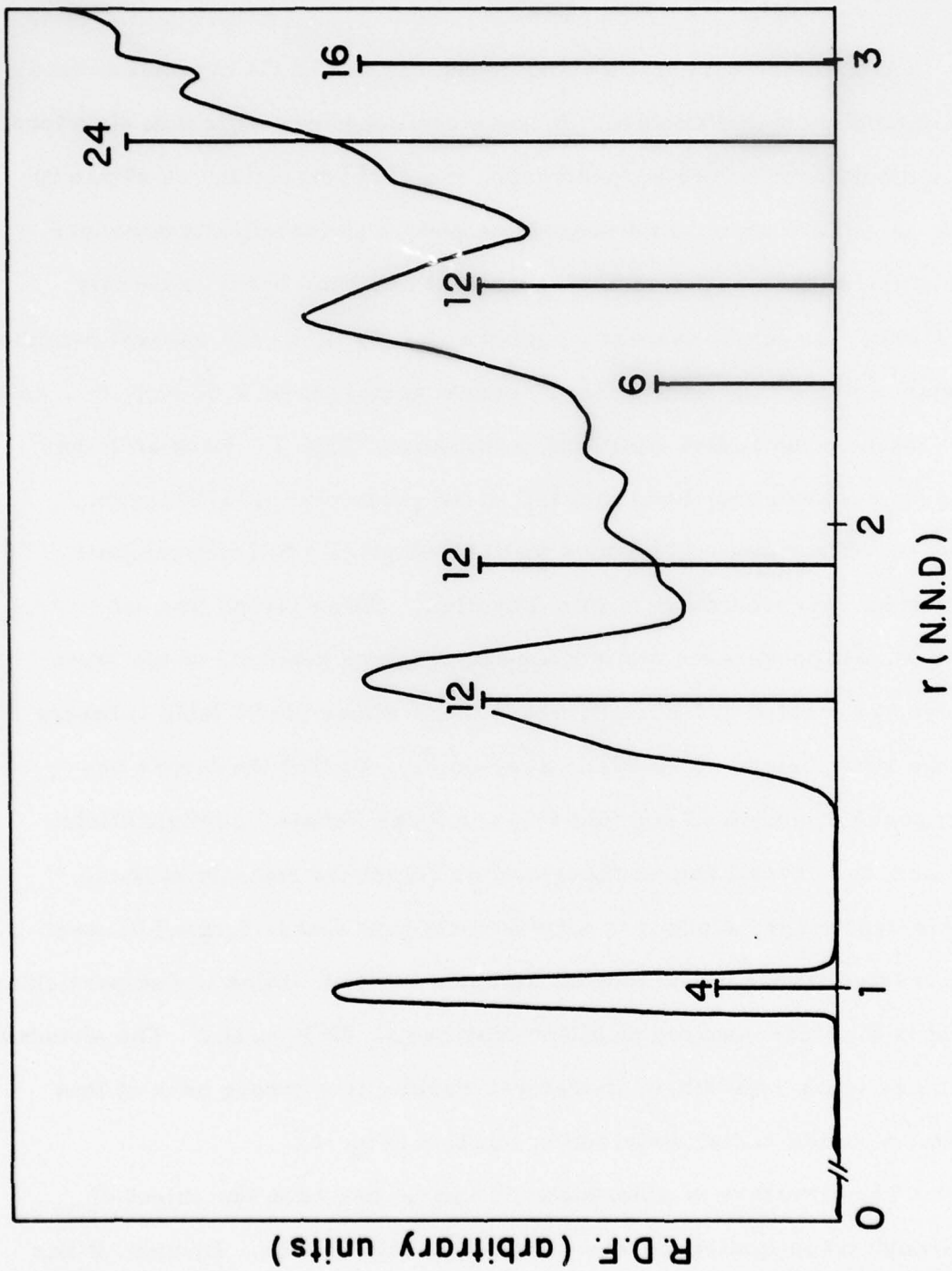


Figure 1

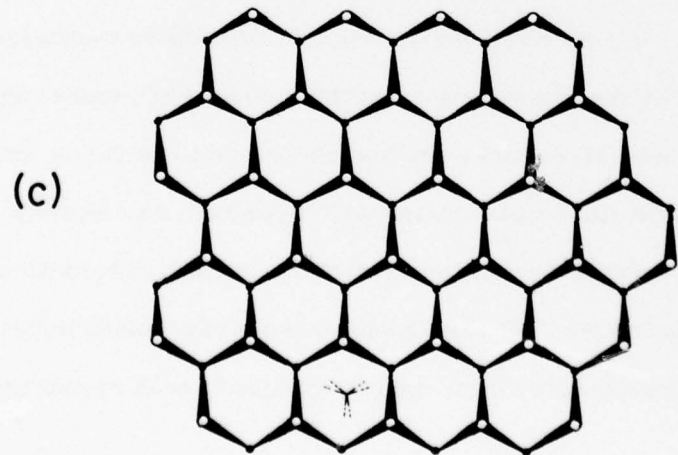
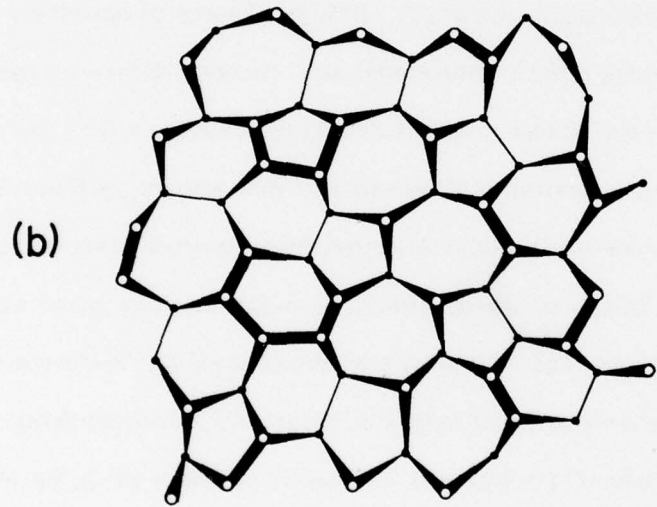
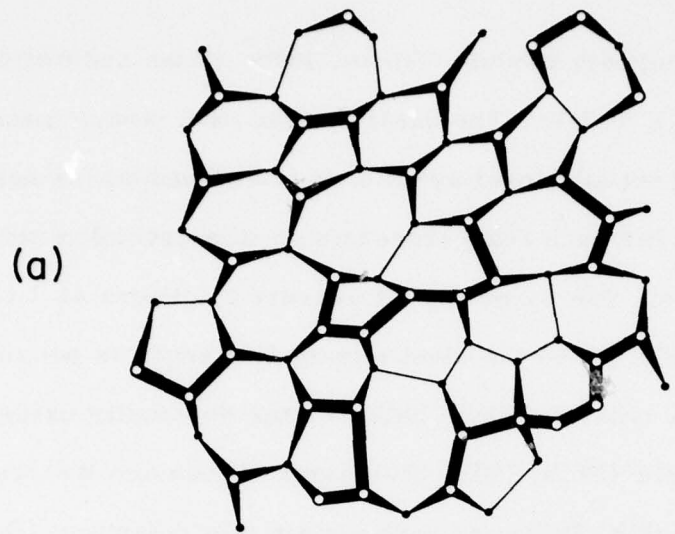


Figure 2

a continuous random network model (Moss, 1973; Moss and Adler, 1973; Paul and Connell, 1974). The basic feature of a random network is the total absence of translational symmetry, combined with a nearest neighbor environment for each atom close to that of a crystal of the same composition, i. e., for Si or Ge: 4 nearest neighbors at 1 N.N.D., and the bond angles as close to the ideal tetrahedral angle as possible. Several models of this type have been built, either physically using plastic tetrahedral units (Polk, 1971; Steinhardt, Alben and Weaire, 1974; Connell and Temkin, 1974), or with the aid of a computer (Boudreaux, Polk and Duffy, 1974; Shevchik and Paul, 1972). Their properties are in agreement with the experimental observations: density close to that of the crystal, no dangling bonds, bond angle distortion less than 20° (r. m. s. $\sim 10^\circ$), and a radial distribution function similar to the one shown in Fig. 1.

The first and second peaks of the amorphous radial distribution function are similar to those of the crystal: 4 nearest neighbors at 1 N.N.D., and 12 next-nearest neighbors at distances spread around 1.63 N.N.D. depending on the bond angle distortion. The striking difference between the two distributions is the third peak at 1.92 N.N.D., which is very strong in the crystal but almost totally smeared out in the amorphous structure. As pointed out above, this distance corresponds to the diagonal distance in the chair-type sixfold rings which make up the crystal. The amorphous structure, on the other hand, is made up of a mixture of five- to eightfold rings, in various proportions, shapes or degrees of distortion depending on the particular model. Despite these differences in ring statistics, all the random networks constructed have similar radial distribution functions, which indicates that replacing most

of the chair-type sixfold rings by any mixture of different ones will result in a disappearance of the third-nearest neighbor peak.

Based on these observations, the following phase-specific construction rules can be identified:

(i) the chair-type sixfold ring which makes up the diamond cubic structure is characteristic of the crystalline phase;

(ii) the virtual disappearance of these chair-type rings and their replacement by a mixture of different ones is characteristic of the amorphous phase.

CONSTRUCTION OF THE INTERFACE MODEL

The model has been constructed with the same plastic units used for bulk random networks (made by Rinco Instrument Co., Greenville, Ill.). The bonds made by these units have some flexibility which allows bond angle distortion, but are rigid enough to prevent distortions above $\sim 25^\circ$.

The description of the diamond cubic structure as a stacking of (111) layers shows clearly that the crystal can be terminated conveniently between two of these layers. Therefore, following the general procedure outlined above, it was decided to start the interface construction with the crystalline phase. A crystal consisting of two (111) layers was constructed and was terminated such that the atoms nearest to the boundary plane had one unsatisfied bond out of the plane, parallel to the [111] direction. The two layers will be designated from here on as the "1st" (closest to the boundary plane) and "2nd"

crystalline layer (see Fig. 2c). They contain 64 and 62 atoms, respectively.

At this point, the following construction rules were used in order to make the transition to the random network amorphous phase. Most important is the change in the phase-specific construction rule, which, as discussed above, consists of making the chair-type sixfold rings disappear. Specifically, this was done here by:

(i) giving preference, as much as possible within the strain limitations, to the construction of any other type of ring over a chair-type sixfold one.

Furthermore, a number of other construction rules, common to both phases were also used:

- (ii) satisfying all the bonds;
- (iii) keeping a unique nearest neighbor distance;
- (iv) minimizing the bond angle distortion.

Since bending a bond is much easier than breaking or stretching it, these last three rules form a simple energy minimization procedure. They were the criterion for choosing one type of ring over another when replacing a chair-type ring.

Since half the atoms in the first crystalline layer had at this point still one open bond, perpendicular to the plane, it was decided to continue the construction by satisfying all these bonds first. This resulted in the creation of what will be called from here on the "1st amorphous layer" (see Fig. 2b). Topologically, it is a two-dimensional structure: each of the 67 atoms, except for the layer edges of course, has three bonds with atoms in the 1st amorphous layer and a fourth bond

connecting it either downwards with the 1st crystalline layer, or upwards with the 2nd amorphous layer (to be built later).

It consists of a mixture of five-, six- and sevenfold rings. Only a few of the sixfold rings approach the "chair" configuration. Most of them have either a "boat" or a distorted configuration. It is clear from Fig. 2b that the new layer has no translational symmetry and is thus truly "amorphous". So, it seems that the particular choice of phase-specific rules made above was indeed sufficient to make the transition from crystalline to amorphous. It is interesting to note that after a few non-chair type rings have been constructed (~ 15 atoms) it was no longer necessary to pay special attention to rule (i), i. e., keep avoiding chair configurations. Once amorphousness was introduced by creating a few noncrystalline rings, adherence to the general rules (ii) - (iv) was sufficient to prevent the reappearance of crystallinity.

The second amorphous layer, formed by satisfying all the loose bonds of the first amorphous layer out of its topological plane, contains 73 atoms and is shown in Fig. 2a. Again, there was no problem keeping the structure amorphous by simply using rules (ii) - (iv). Topologically, this layer is also three-connected, except for one atom near the edge which has all four bonds in the topological plane.

Based on our previous experience with physical model building, it was felt that at this stage the construction had become qualitatively similar, in terms of the number of choices available and the amount of strain introduced, to that of a bulk random network. Therefore, it was deemed unnecessary to add any more layers. Suffice it to point out that the model can be extended in all directions without any problem. Figure 3 shows two views of the completed structure.

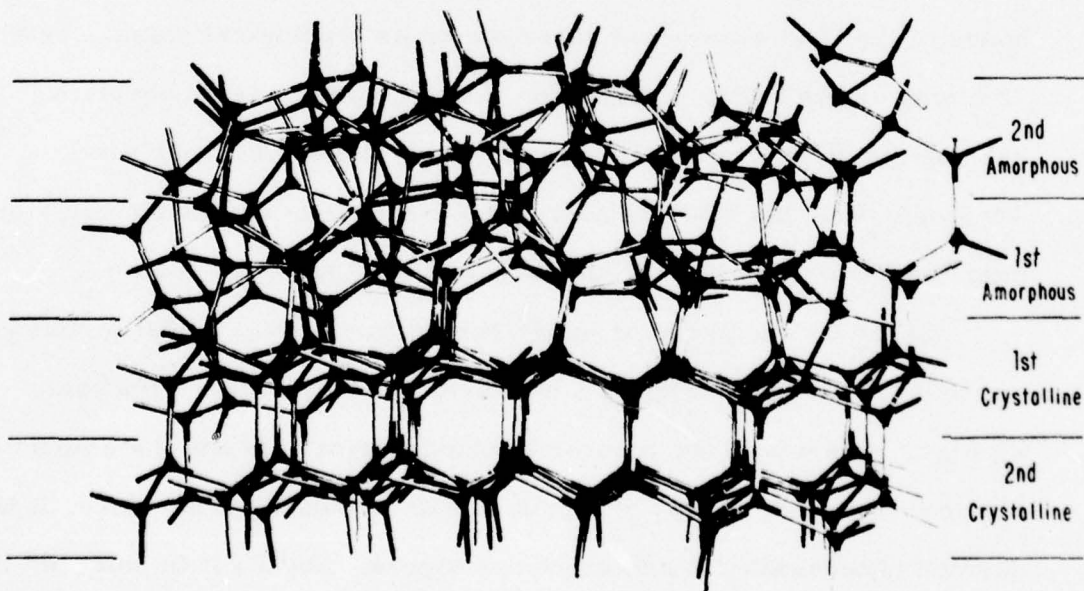
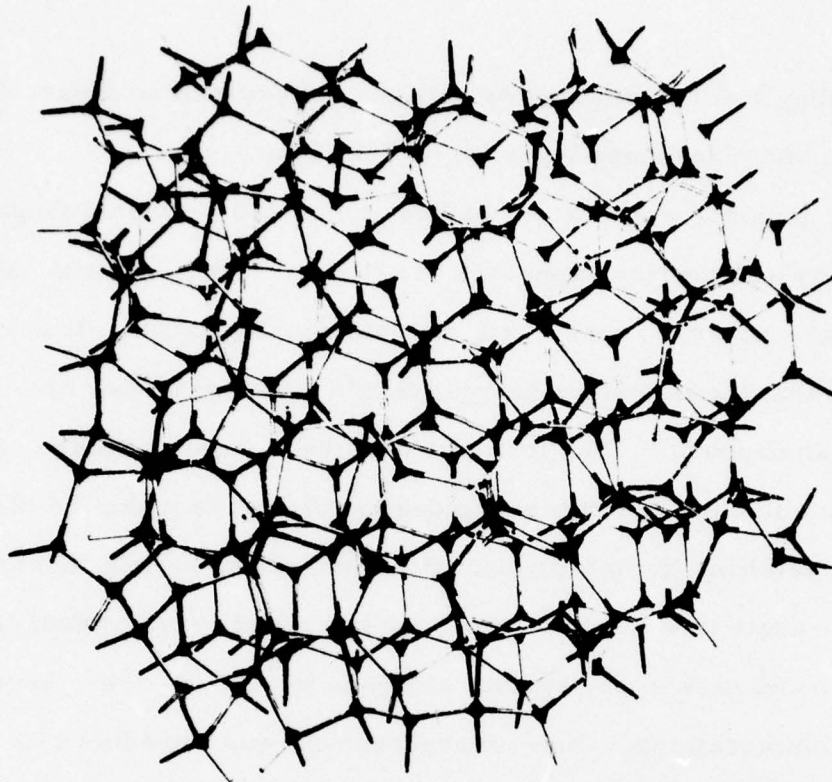


Figure 3

MEASUREMENTS AND OBSERVATIONS

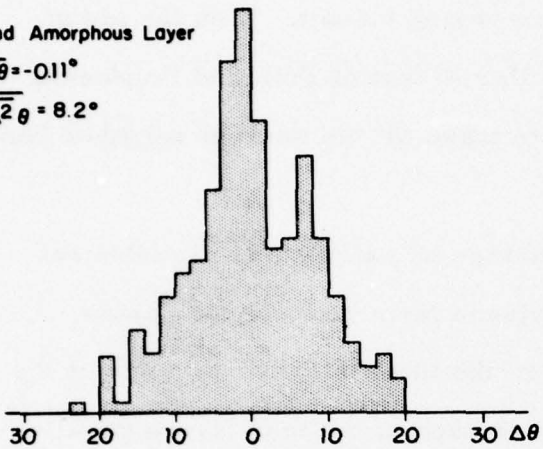
The coordinates of the 266 atoms were measured by a triangulation method, using a laser mounted on a surveying transit. With the aid of the computer, using an algorithm similar to that of Polk and Boudreaux (1973), the coordinates were refined to make all the nearest neighbor bond lengths exactly equal.

The bond angle distortions could then be calculated. To illustrate the variation of the distortion with distance from the boundary plane, Fig. 4 shows the deviations ($\Delta\theta$) from the ideal tetrahedral angle of the bond angles associated with the atoms in each of the four layers parallel to the boundary. There are six angles between the four bonds of each atom; however, bond angles with an unsatisfied bond (at the model's outer surface) have obviously not been taken into account. The mean bond angle deviation $\overline{\Delta\theta}$ is close to zero in all four layers and the distributions are roughly symmetrical about the origin. The standard deviation $\sqrt{\overline{\Delta\theta^2}}$, which is a measure of the bond angle distortion, is 10.0° and 8.2° for the 1st and 2nd amorphous layer; 8.6° and 4.8° for the 1st and 2nd crystalline layer, respectively. Since this value for the bulk crystalline and amorphous phase is 0° and 9.1° , respectively, it becomes clear that the creation of the interface results in an excess distortion of the bond angles near the boundary plane. The excess strain energy associated with this distortion contributes to the surface tension. The 2nd crystalline layer is less distorted than the 1st one and it seems plausible that the excess distortion will keep decreasing with increasing distance from the boundary. The 1st amorphous layer is more

2nd Amorphous Layer

$$\overline{\Delta\theta} = -0.11^\circ$$

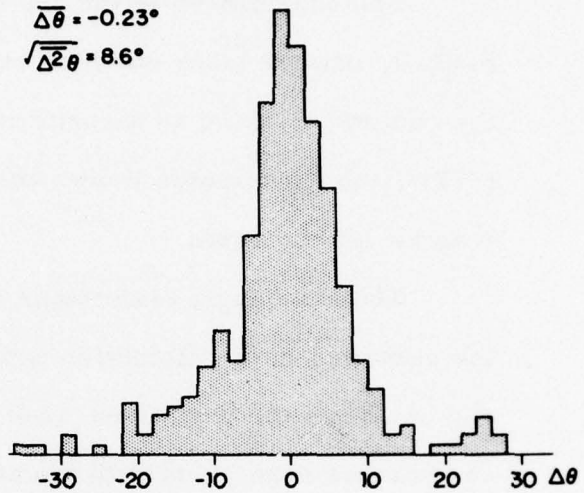
$$\sqrt{\Delta^2\theta} = 8.2^\circ$$



1st Crystalline Layer

$$\overline{\Delta\theta} = -0.23^\circ$$

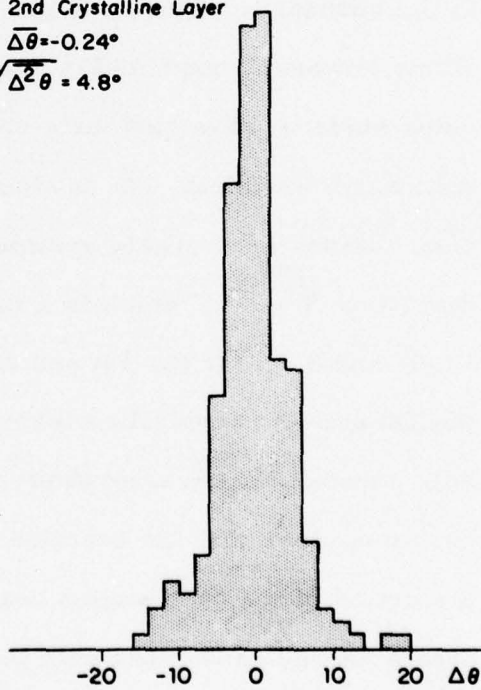
$$\sqrt{\Delta^2\theta} = 8.6^\circ$$



2nd Crystalline Layer

$$\overline{\Delta\theta} = -0.24^\circ$$

$$\sqrt{\Delta^2\theta} = 4.8^\circ$$



1st Amorphous Layer

$$\overline{\Delta\theta} = -0.34^\circ$$

$$\sqrt{\Delta^2\theta} = 10.0^\circ$$

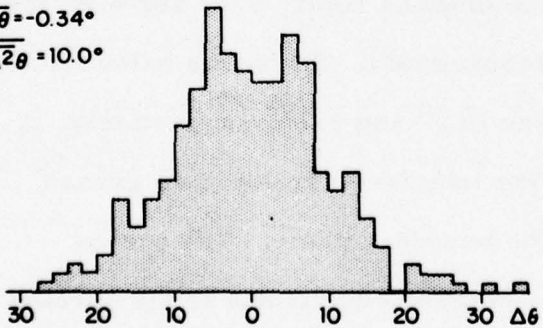


Figure 4

distorted than the bulk amorphous phase. The 2nd amorphous layer, however, seems to be less distorted; there is no obvious physical explanation for this, and it is probably an artifact caused by the large number of unsatisfied surface bonds in this layer; enlarging the model would probably result in a slight increase of the distortion. Suffice it to point out that also in this respect the 2nd amorphous layer, in agreement with the observations during the construction of the model, is quite similar to the bulk amorphous phase.

To illustrate the variation of the structure with distance from the boundary; Fig. 5 shows the radial distribution functions of the four interface layers. Since only distances between atoms in the same layer are used, these R. D. F. 's are close to two-dimensional and should be defined as $2\pi r \rho'(r)$. The average distribution is $2\pi r \rho'_0$ (i. e., linear in r), where ρ'_0 is the average number of atoms per unit area of the layer. Since the nearest neighbor distances and nearest neighbor coordination are nearly the same for all atoms in the model, their atomic volumes, defined e. g., by a Voronoi construction, are expected to be almost identical. (The difference between the bulk crystalline and amorphous atomic volume is only $\sim 1\%$). Therefore, ρ'_0 was taken to be $.866 \text{ atoms (NN D)}^{-2}$, which is the planar density of the crystalline (111) planes. Since $\rho'(r)$ is defined for an infinite layer, it was necessary to correct for the finite size of the layers by introducing a size factor $F(r, \text{size})$, which is defined as the ratio between the number of pairs at a distance between r and $r + dr$ per atom in a layer of finite size (measured on the model) and the number of pairs at the same distance per atom in an infinite layer ($= 2\pi r \rho'(r)$). Expressions for

$F(r, \text{size})$ are available only in three dimensions, but it is easy to derive an expression in two dimensions using the same basic approach. It is assumed that the shape of the finite layers can be approximated by a circle with effective outer radius R . Formally, this means that the expression for the atom positions in a finite size layer can be obtained by multiplying the expression for an infinite cluster by a shape factor $S(r) = 1$ for $r \leq R$; $S(r) = 0$ elsewhere. It is straightforward to show that the size factor $F(r, R)$ is the autocorrelation function of the shape factor $S(r, R)$ or:

$$F(r, R) = \frac{1}{\pi} \left[2 \arctan \sqrt{\left(\frac{2R}{r}\right)^2 - 1} - \frac{r}{R} \sqrt{1 - \left(\frac{r}{2R}\right)^2} \right].$$

After this correction was made, the R. D. F. 's do indeed approach the linear average distribution at large distances and the number of nearest neighbors, obtained by integrating the first peak, is indeed very close to 3.

The R. D. F. of a perfect, undistorted crystalline (111) layer consists of a series of deltafunctions with positions and area as indicated at the top edge of Fig. 5c. The peaks in the R. D. F. 's of the 1st and 2nd crystalline layers have been broadened by the bond angle distortion, but they are in the right positions and have the right integrated peak area. The peaks of the 2nd crystalline layer are sharper than those of the 1st layer, which reflects the lower bond angle distortion. To compare the structure of the two-dimensional 2nd amorphous layer to that of the three-dimensional bulk amorphous phase, their respective pair distribution functions $w'(r) = \rho'(r)/\rho'_0$ and $w(r) = \rho(r)/\rho_0$ are

shown on Fig. 6. Because of the difference in their normalization the two functions can only be compared qualitatively, but their similarity is clear. The absence of a strong peak at 1.92 N. N. D. in $w'(r)$ reflects the phase-specific construction rule which forbids the chair-type configurations on the amorphous side of the boundary.

A final observation is concerned with the degree of localization, perpendicular to the boundary, of the amorphous layers near the interface. The layer localization can be characterized by the maximum distance normal to the boundary plane between any two of its atoms. For example, for the crystalline (111) planes, this is simply the puckering height: $1/3$ N. N. D. For the 1st and 2nd amorphous layers this was measured, after correcting for a slight overall bend in the model, to be 0.74 N. N. D. and 1.03 N. N. D., respectively. This means that the degree of localization decreases with increasing distance from the boundary, i. e.: the structure becomes more "random" in the direction normal to the boundary. The 2nd amorphous layer, however, is still more localized than a totally random distribution of the atoms would be, as can be seen from the following argument: since it is possible to establish a one-to-one correspondence between the atoms of subsequent layers, the planar density of all the layers must be the same, i. e., equal to that of a crystalline (111) plane. Since all the atoms, because of their identical nearest neighbor distance and coordination, have the same atomic volume, the spacing normal to the boundary between subsequent layers must on the average be the (111) spacing, or $4/3$ N. N. D. If the atoms in the 2nd amorphous layer were not localized at all, one would therefore expect this value to be the maximum normal distance

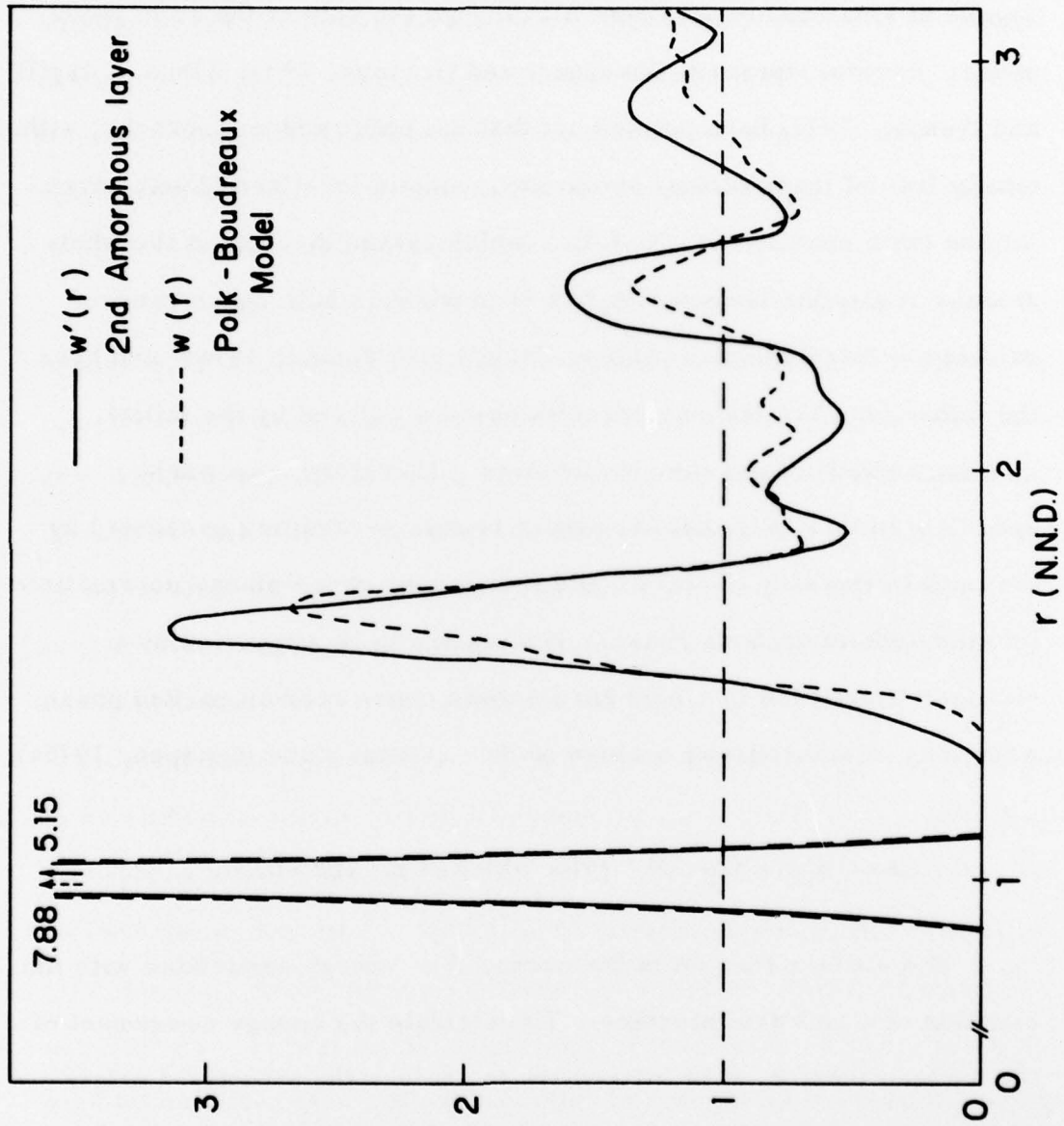


Figure 6

between any two of its atoms. Whether or not the localization of subsequent layers would disappear if the model were enlarged is open to speculation. It would not be totally surprising, however, if a certain degree of localization persisted all through the bulk of the amorphous phase. Several workers (Chaudhari and Graczyk, 1974; Alben, Cargill and Wenzel, 1976) have pointed out that the bulk random networks, although totally free of translational symmetry, contain localized planar correlations (with spacing $4/3$ N. N. D.) which extend throughout the whole model. A similar observation has been made in bulk dense random packings of hard spheres (Alben, Cargill and Wenzel, 1976), and here the indications are that the correlations are induced by the initial boundary conditions of the construction. Therefore, one might speculate in this case that the planar boundary condition presented by the initial crystalline layers could induce long range planar correlations into the bulk amorphous phase. This seems to be supported by a similar observation in a bulk hard sphere dense random packed phase, when it is interfaced with a close packed crystal plane (Spaepen, 1975a).

CALCULATION OF THE SURFACE TENSION

The surface tension is the excess free energy associated with the creation of a unit area interface. To calculate the energy component of the surface tension, it is instructive to analyze the structural origin of the energy difference between bulk crystalline and amorphous Ge.

The enthalpy of crystallization (ΔH_c) of amorphous Ge is 2.75 kcal/mole or 29.8 meV/valence electron (Chen and Turnbull, 1969).

As discussed by Polk (1971a), there are three possible contributions to the higher energy of the amorphous phase: strain energy due to bond stretching (E_s), strain energy due to bond bending (E_b), and the energy associated with the relative orientation of neighboring tetrahedra (E_d).

The first contribution (E_s) is zero for random network models with a unique nearest neighbor distance equal to the crystalline one. The second contribution has been calculated by Moss, Alben, Adler and de Neufville (1973) to be

$$E_b = \frac{3}{4} kd^2 \overline{\Delta^2 \theta} \quad \text{per electron} \quad (1)$$

where

- $\Delta^2 \theta$: the mean square bond angle deviation
= $(9.1^\circ)^2 = (0.16)^2$ for the Polk-Boudreaux model
- d : the nearest neighbor distance
= 2.43×10^{-10} m for Ge
- k : the force constant for bond bending
= 2.4 Nm^{-1} for Ge, derived from phonon-dispersion curves.

This gives

$$E_b = 17.05 \text{ meV/electron} \quad .$$

The third contribution comes from the difference in relative rotation between neighboring tetrahedra; in the crystal, all neighboring tetrahedra are in the 'staggered' configuration, which is the one of

lowest energy; in the amorphous phase there exists a continuous distribution of all orientations between 'staggered' and 'eclipsed', which results in a higher energy. It is difficult to calculate this energy independently, and therefore it will be assumed that it simply is the balance to make the energies add up to ΔH_c , or $E_d = 12.75$ meV/electron.

The energy contribution to the surface tension can be calculated using the same approach. The results for Ge are summarized in Table 1, which shows the contribution of each of the four layers of the model. The strain energy associated with the bond angle distortion, E_b , is calculated with Equation (1). N_d is the average number of electrons per atom participating in a bond that connects two tetrahedra whose relative orientation is not the crystalline 'staggered' one. In the two amorphous layers, all four of each atom's electrons are in this case, while in the 2nd crystalline layer there are none. In the 1st crystalline layer, each atom has 3 electrons participating in bonds within the layer; the fourth electron participates in a bond with either the 2nd crystalline or 1st amorphous layer; since only the bonds to the 1st amorphous layer connect tetrahedra which are not in the 'staggered' orientation and since half the atoms in the layer are connected this way, $N_d = 0.5$ for this layer. If it is now assumed that the distribution of the relative orientations of the neighboring tetrahedra which are not in the 'staggered' configuration is the same as in the bulk amorphous phase, the resulting contribution to the energy is $E_d = N_d E_d(\text{bulk}) = N_d \times 12.75$ meV/atom. Both contributions are added up to give the total energy: $E = 4E_b + E_d$. The excess energy ΔE is the difference

TABLE 1

Layer #	$\sqrt{\Delta^2 \theta}$ ($^\circ$)	E_b (meV/ electron)	N_d	E_d (meV/ atom)	E (meV/ atom)	ΔE (meV/ atom)
2nd amorphous	8.2	13.78	4	51.00	106.11	0
1st amorphous	10.0	20.67	4	51.00	133.69	14.38
1st crystalline	8.6	15.26	0.5	6.33	67.43	67.43
2nd crystalline	4.8	4.67	0	0	18.66	18.66
TOTAL						100.47

between the energy of the interfacial layers (E) and the energy of the respective bulk phases. For the crystalline layers, the bulk value is of course zero, so that $\Delta E = E$. For the amorphous layers, the bulk value is $\Delta H_c = 119.31 \text{ meV/atom}$ and $\Delta E = E - \Delta H_c$. For the 2nd amorphous layer, this results in a negative value due to a bond angle distortion (8.2°) which is apparently lower than the bulk value (9.1°). However, as discussed in the previous section, this unphysical result is probably an artifact that would disappear if another layer were added to the model. Therefore, because the 2nd amorphous layer is quite similar to the bulk amorphous phase in many other respects, its excess energy is simply set equal to zero. Adding up the contributions of the four layers gives the energy part of the surface tension: 100.47 meV/atom in the boundary plane. The area per atom in a Ge (111) plane is $6.82 \times 10^{-20} \text{ m}^2$, which means that the surface tension can be written as:

$$\sigma \geq 0.235 \text{ J m}^{-2}$$

This value for the surface tension is a lower limit. If more crystalline and amorphous layers were added to the model, they would probably also have some bond angle distortion, but their contribution to the strain energy would be small since the energy depends on the square of the distortion which decreases with increasing distance from the boundary. Another possible contribution to the surface tension is the entropy due to the localization of the amorphous layers near the boundary. However, the configurational entropy of these random networks is so low (0.2 k per atom is an upper limit (Spaepen, 1974))

that even if one complete amorphous layer would lose all its configurational entropy, the resulting change in the surface tension at room temperature would be at most 5%.

DISCUSSION AND CONCLUSIONS

1. It has been demonstrated that an interface can be constructed between the amorphous and crystalline phases of tetrahedrally coordinated materials by following the general procedure of changing the appropriate phase-specific construction rules.

2. The resulting interface has no broken bonds and this corresponds to a state of lowest energy. Breaking a bond in Ge costs 1.63 eV (Pauling, 1960), while the energy associated with forming the interface without broken bonds is .100 eV/atom in the boundary plane. This means that breaking a bond in the interface would be energetically favorable if it would relieve the strain in approximately 60 atoms around it; it was clear from the model building experience that this could never be the case. Whether or not the interfaces in crystallization experiments resemble this ideal lowest energy model depends on the extent to which loose bonds have been annealed out after preparation of the samples. It seems probable that the model would be most applicable to slow crystal growth processes, or growth in pre-annealed samples.

3. The surface tension is mainly energetic in origin. When normalized in terms of the heat of transformation per atom Δh_c , the surface tension can be written as $\sigma \geq 0.84 \Delta h_c / \text{atom}$ in the boundary

plane. This value is comparable to that calculated for the surface tension between a monatomic hard-sphere like crystal and its melt at the melting point $\sigma = 0.85 \Delta h_f/\text{atom}$ in the boundary plane. The crystal-melt surface tension, however, is negentropic in origin, which means that the surface tension scales with absolute temperature, while the amorphous-crystalline surface tension never falls below the value of its energetic component. This value is large enough to suppress homogeneous nucleation of Ge crystals in the amorphous covalent phase (Turnbull, 1969). It is difficult to check this experimentally, since most amorphous films have many impurities which can act as heterogeneous nucleation sites. The fact that other network formers (SiO_2 , Se) where one would expect a similar energetic surface tension, are good glass formers is consistent with this calculation, although in these cases it is difficult to separate the effects of jump frequency and surface tension on homogeneous nucleation.

4. The model makes it possible to be more specific about the problem of putting together an assembly of randomly oriented microcrystallites or other regular microclusters ('amorphons') by connecting them with a random network matrix (Hoare, 1976). Replacing part of a random network with a spherical crystallite of diameter d results in a lowering of the energy, since the crystallite is initially unstrained, by $\pi d^3 \Delta h_c / 6 \bar{v}$ (\bar{v} is the atomic volume), and an increase in energy due to the surface tension of the newly created interface (assumed isotropic) by $\pi d^2 (0.84 \Delta h_c) / (\bar{v})^{2/3}$. The new system will have the same energy as the random network if the two contributions are equal or: $d = 5(\bar{v})^{1/3}$. Therefore, if one were to construct a microcrystalline

composite model that is energetically equivalent to the random network model for amorphous Ge, the crystallite size would be 14 \AA . The interface model shows that the 2nd amorphous layer begins to resemble the bulk phase; therefore, in order to make the transition between two randomly oriented crystallites at least three amorphous layers must be constructed between them; the middle one of those three layers approaches the bulk structure and can therefore be shared by both crystallites as their 2nd amorphous interface layer. The spacing of the interface layers is the crystalline (111) spacing d_{111} . The distance between the centers of two adjoining crystallites is therefore at least $d + 3d_{111}$. In the case of Ge, this means that the amorphous matrix necessary to join the crystallites takes up more than 80% of the volume. The only way to decrease this amount substantially is by arranging the crystallites or microclusters in a highly correlated way (Gaskell, 1975).

5. The model can be a starting point for understanding the topology and energetics of the crystallization process. It is clear that in order to make any topological changes in the model at all, it is necessary to break and reconnect the bonds. Preliminary investigations seem to indicate that it is possible to make major topological rearrangements by breaking one bond and propagating the resulting loose ends through the network; some of the intermediate configurations necessary for propagation of the loose bond require local extra strain. This strain energy could explain the difference between the energies required for bond breaking (1.63 eV for Ge and 1.82 eV for Si (Pauling, 1960)) and the activation energies of the crystallization process (2.0 eV for Ge (Csepregi, Kullen, Mayer and Sigmon, 1977) and 2.3 eV for Si (Csepregi, Mayer and Sigmon, 1975)). This question obviously needs further investigation.

ACKNOWLEDGEMENTS

I would like to thank Prof. D. Turnbull for his encouragement and help during the course of this work. Discussions with Prof. J. W. Mayer and Dr. G. A. N. Connell have been very useful.

This work has been supported by the Office of Naval Research under Contract No. N00014-77-C-0002 and by the National Science Foundation under Contract No. NSF-DMR76-0111.

I also want to acknowledge a postdoctoral Fellowship from the I. B. M. Corporation.

REFERENCES

- Alben, R., Cargill III, G. S., and Wenzel, J., 1976, *Phys. Rev.*, B13, 835.
- Barna, A., Barna, P. B., and Pocza, J. F., 1972, *J. Non-Crystalline Solids*, 8-10, 36.
- Bernal, J. D., 1964, *Proc. Roy. Soc.*, 280A, 299.
- Boudreaux, D. S., Polk, D. E., and Duffy, M. G., 1974, *Proceedings of the International Conference on Tetrahedrally Bonded Amorphous Semiconductors*, Yorktown Heights, N. Y., A. I. P. Conference Proceedings 20, p. 206.
- Bourgoin, J. C., and Germain, P., 1975, *Phys. Lett.*, 54A, 444.
- Chaudhari, P., and Graczyk, J. F., 1974, *Proceedings of the Fifth International Conference on Amorphous and Liquid Semiconductors*, Garmisch, edited by J. Stuke and W. Brenig (London: Taylor and Francis Ltd.), p. 59.
- Chen, H. S., and Turnbull, D., 1969, *J. Appl. Phys.*, 40, 4214
- Chik, K. P., and Lim, P. K., 1975, *Thin Sol. Films*, 35, 45.
- Czepregi, L., Kullen, R. P., Mayer, J. W., and Sigmon, T. W., 1977, *Sol. St. Comm.*, 21, 1019.
- Csepregi, L., Mayer, J. W., and Sigmon, T. W., 1975, *Phys. Lett.*, 54A, 157.
- Finney, J. L., 1970, *Proc. Roy. Soc.*, 319A, 479.
- Gaskell, P. H., 1975, *Phil. Mag.*, 32, 211.
- Germain, P., Squelard, S., Bourgoin, J. C., and Gheorghiu, A., 1975, *J. Non-Crystalline Solids*, 23, 93.
- Gleiter, H., and Chalmers, B., 1972, *Prog. Mat. Sci.*, Chalmers, Christian and Massalski eds., (Pergamon), 16, pp. 1-12.
- Hoare, M., 1976, *Ann. N. Y. Acad. Sci.*, 279, 186.
- Moss, S. C., 1973, *Proceedings of the Fifth International Conference on Amorphous and Liquid Semiconductors*, Garmisch, edited by J. Stuke and W. Brenig (London: Taylor and Francis Ltd.), p. 17.

- Moss, S. C., and Adler, D., 1973, *Comments Solid St. Phys.*, 5, 47.
- Moss, S. C., Alben, R., Adler, D., and de Neufville, J. P., 1973, *J. Non-Crystalline Solids*, 13, 185.
- Paul, W., and Connell, G. A. N., 1974, *Physics of Structurally Disordered Solids*, edited by S. S. Mitra, (Plenum, N. Y.), p. 45.
- Pauling, L., 1960, *Nature of the Chemical Bond*, (Cornell University Press, Ithaca, N. Y.), p. 85.
- Polk, D. E., 1971, *J. Non-Crystalline Solids*, 5, 365; 1971a, Thesis, Harvard University, pp. 5-23.
- Polk, D. E., and Boudreaux, D. S., 1973, *Phys. Rev. Lett.*, 31, 92.
- Shevchik, N. J., and Paul, W., 1972, *J. Non-Crystalline Solids*, 8-10, 381.
- Spaepen, F., 1974, *Phil. Mag.* 30, 417; 1975, *Acta Met.*, 23, 729; 1975a, Thesis, Harvard University, p. 112.
- Spaepen, F., and Meyer, R. B., 1976, *Scripta Met.*, 10, 257.
- Steinhardt, P., Alben, R., and Weaire, D., *J. Non-Crystalline Solids*, 15, 199.
- Turnbull, D., 1969, *Contemp. Phys.*, 10, 473.

FIGURE CAPTIONS

- Fig. 1: Radial distribution function of the Polk-Boudreaux (1973) tetrahedrally coordinated random network structure. The number and positions of the neighbors in the diamond cubic lattice are indicated by the vertical lines.
- Fig. 2: Topology of the four layers in the interface model. The circles and dots represent atoms whose fourth bond connects, respectively, to the layer above or below.
- (a) the 2nd amorphous layer;
 - (b) the 1st amorphous layer;
 - (c) the 1st crystalline layer; the position of the 2nd crystalline layer is indicated.
- Fig. 3: Top and side view of the completed interface model; the four layers are indicated.
- Fig. 4: The distribution of the bond angle deviations for the four interface layers.
- Fig. 5: The radial distribution functions for the four interface layers. The dashed line corresponds to the average density. The number and positions of the interatomic distances in an undistorted (111) layer are indicated on the top edge of (c).
- Fig. 6: Comparison of the pair distribution functions of a bulk random network and the 2nd amorphous layer.

Defense Documentation Center
 Cameron Station
 Alexandria, Virginia 22314 (12)

Office of Naval Research
 Department of the Navy
 Attn: Code 471 (3)
 Code 105 (6)
 Code 470

Director
 Office of Naval Research
 Branch Office
 495 Summer Street
 Boston, Massachusetts 02210

Director
 Office of Naval Research
 Branch Office
 516 South Clark Street
 Chicago, Illinois 60605

Office of Naval Research
 San Francisco Area Office
 760 Market Street, Room 447
 San Francisco, California 94102

Naval Research Laboratory
 Washington, D. C. 20390
 Attn: Code 6000
 Code 6100
 Code 6300
 Code 6400
 Code 2627 (6)

Attn: Mr. F. S. Williams
 Naval Air Development Center
 Code 302
 Warminster, Pennsylvania 18974

Naval Air Propulsion Test Center
 Trenton, New Jersey 08628
 Attn: Library

Naval Weapons Laboratory
 Dahlgren, Virginia 22448
 Attn: Research Division

Naval Construction Battalion
 Civil Engineering Laboratory
 Port Hueneme, California 93043
 Attn: Materials Division

Naval Electronics Laboratory Center
 San Diego, California 92152
 Attn: Electronic Materials Sciences Div.

Naval Missile Center
 Materials Consultant
 Code 312-1
 Point Mugu, California 93041

Commanding Officer
 Naval Ordnance Laboratory
 White Oak
 Silver Spring, Maryland 20910
 Attn: Library

Naval Ship R. and D. Center
 Materials Department
 Annapolis, Maryland 21402

Naval Undersea Center
 San Diego, California 92132
 Attn: Library

Naval Underwater System Center
 Newport, Rhode Island 02840
 Attn: Library

Naval Weapons Center
 China Lake, California 93555
 Attn: Library

Naval Postgraduate School
 Monterey, California 93940
 Attn: Materials Sciences Dept.

Naval Air Systems Command
 Washington, D. C. 20360
 Attn: Code 52031
 Code 52032
 Code 320

Naval Sea System Command
 Washington, D. C. 20362
 Attn: Code 035

Naval Facilities
 Engineering Command
 Alexandria, Virginia 22331
 Attn: Code 03

Scientific Advisor
 Commandant of the Marine Corps
 Washington, D. C. 20380
 Attn: Code AX

Naval Ship Engineering Center
 Department of the Navy
 Washington, D. C. 20360
 Attn: Director, Materials Sciences

Army Research Office
 Box CM, Duke Station
 Durham, North Carolina 27706
 Attn: Metallurgy and Ceramics Div.

Army Materials and Mechanics
 Research Center
 Watertown, Massachusetts 02172
 Attn: Res. Programs Office (AMXMR-P)

Commanding General
 Department of the Army
 Frankford Arsenal
 Philadelphia, Pennsylvania 19137
 Attn: ORDBA-1320

Office of Scientific Research
 Department of the Air Force
 Washington, D. C. 20333
 Attn: Solid State Div. (SRPS)

Aerospace Research Labs
 Wright-Patterson AFB
 Building 450
 Dayton, Ohio 45433

Air Force Materials Lab (LA)
 Wright-Patterson AFB
 Dayton, Ohio 45433

NASA Headquarters
 Washington, D. C. 20546
 Attn: Code RRM

NASA
 Lewis Research Center
 21000 Brookpark Road
 Cleveland, Ohio 44135
 Attn: Library

National Bureau of Standards
 Washington, D. C. 20234
 Attn: Metallurgy Division
 Inorganic Materials Division

Atomic Energy Commission
 Washington, D. C. 20545
 Attn: Metals and Materials Branch

Defense Metals and Ceramics
 Information Center
 Battelle Memorial Institute
 505 King Avenue
 Columbus, Ohio 43201

Director
 Ordnance Research Laboratory
 P. O. Box 30
 State College, Pennsylvania 16801

Director Applied Physics Lab.
 University of Washington
 1013 Northeast Fortieth Street
 Seattle, Washington 98105

Metals and Ceramics Division
 Oak Ridge National Laboratory
 P. O. Box X
 Oak Ridge, Tennessee 37830

Los Alamos Scientific Lab.
 P. O. Box 1663
 Los Alamos, New Mexico 87544
 Attn: Report Librarian

Argonne National Laboratory
 Metallurgy Division
 P. O. Box 229
 Lemont, Illinois 60439

Brookhaven National Laboratory
 Technical Information Division
 Upton, Long Island
 New York 11973
 Attn: Research Library

Library
 Building 50, Room 114
 Lawrence Radiation Laboratory
 Berkeley, California

Professor G. S. Ansell
 Rensselaer Polytechnic Institute
 Dept. of Metallurgical Engineering
 Troy, New York 12181

Professor H. K. Birnbaum
 University of Illinois
 Department of Metallurgy
 Urbana, Illinois 61801

Dr. E. M. Breiman
 United Aircraft Corporation
 United Aircraft Research Lab.
 East Hartford, Connecticut 06108

Professor H. D. Brody
 University of Pittsburgh
 School of Engineering
 Pittsburgh, Pennsylvania 15213

Professor J. B. Cohen
 Northwestern University
 Dept. of Material Sciences
 Evanston, Illinois 60201

Professor M. Cohen
 Massachusetts Institute of Technology
 Department of Metallurgy
 Cambridge, Massachusetts 02139

Professor B. C. Giessen
 Northeastern University
 Department of Chemistry
 Boston, Massachusetts 02115

Dr. G. T. Hahn
 Battelle Memorial Institute
 Department of Metallurgy
 515 King Avenue
 Columbus, Ohio 43201

Professor R. W. Heckel
 Carnegie-Mellon University
 Schenley Park
 Pittsburgh, Pennsylvania 15213

Dr. David G. Howden
 Battelle Memorial Institute
 Columbus Laboratories
 505 King Avenue
 Columbus, Ohio 43201

Professor C. E. Jackson
 Ohio State University
 Dep. of Welding Engineering
 190 West 19th Avenue
 Columbus, Ohio 43210

Professor G. Judd
 Rensselaer Polytechnic Institute
 Dept. of Materials Engineering
 Troy, New York 12181

Dr. C. S. Kortovich
 TRW, Inc.
 23555 Euclid Avenue
 Cleveland, Ohio 44117

Professor D. A. Ross
 Michigan Technological University
 College of Engineering
 Houghton, Michigan 49931

Professor A. Lawley
 Drexel University
 Dept. of Metallurgical Engineering
 Philadelphia, Pennsylvania 19104

Dr. H. Margolin
 Polytechnic Institute of New York
 333 Jay Street
 Brooklyn, New York 11201

Professor K. Masabuchi
 Massachusetts Institute of Technology
 Department of Ocean Engineering
 Cambridge, Massachusetts 02139

Dr. G. H. Meier
 University of Pittsburgh
 Dept. of Metallurgical and Materials
 Engineering
 Pittsburgh, Pennsylvania 15213

Professor J. W. Morris, Jr.
 University of California
 College of Engineering
 Berkeley, California 94720

Professor K. Ono
 University of California
 Materials Department
 Los Angeles, California 90024

Professor W. F. Savage
 Rensselaer Polytechnic Institute
 School of Engineering
 Troy, New York 12181

Dr. C. Shaw
 Rockwell International Corp.
 P. O. Box 1085
 1049 Camino Dos Rios
 Thousand Oaks, California 91360

Professor O. D. Sherby
 Stanford University
 Materials Sciences Dept.
 Stanford, California 94300

Professor J. Shyne
 Stanford University
 Materials Sciences Department
 Stanford, California 94300

Dr. W. A. Spitzig
 U. S. Steel Corporation
 Research Laboratory
 Monroeville, Pennsylvania 15146

Dr. E. A. Starke, Jr.
 Georgia Institute of Technology
 School of Chemical Engineering
 Atlanta, Georgia 30332

Professor N. S. Stoloff
 Rensselaer Polytechnic Institute
 School of Engineering
 Troy, New York 12181

Dr. E. R. Thompson
 United Aircraft Research Lab.
 400 Main Street
 East Hartford, Connecticut 06108

Professor David Turnbull
 Harvard University
 Division of Engineering and Applied
 Physics
 Cambridge, Massachusetts 02139

Dr. F. W. Wang
 Naval Ordnance Laboratory
 Physics Laboratory
 White Oak
 Silver Spring, Maryland 20910

Dr. J. C. Williams
 Rockwell International
 Science Center
 P. O. Box 1085
 Thousand Oaks, California 91360

Professor H. G. F. Wilsdorf
 University of Virginia
 Department of Materials Science
 Charlottesville, Virginia 22903

Dr. M. A. Wright
 University of Tennessee
 Space Institute
 Dept. of Metallurgical Engineering
 Tullahoma, Tennessee 37388